Magnetic configuration scans during divertor operation of Wendelstein 7-X

T. Andreeva[1], J. Geiger[1], A. Dinklage[1], G. Wurden[2], H. Thomsen[1], K. Rahbarnia[1], J. C. Schmitt[3], M. Hirsch[1], G. Fuchert[1], C. Nührenberg[1], A. Alonso[4], C. D. Beidler[1], M. Beurskens[1], S. Bozhenkov[1], R. Brakel[1], C. Brandt[1], V. Bykov[1], M. Grahl[1], O. Grulke[1], C. Killer[1], G. Kocsis[5], T. Klinger[1], A. Krämer-Flecken[6], S. Lazerson[1], M. Otte[1], N. Pablant[7], J. Schilling[1], E. Trier[8], T. Windisch[1], and the W7-X Team

[1] *Max-Planck-Institute for Plasma Physics, Wendelsteinstrasse. 1, 17491 Greifswald, Germany*

[2] *Los Alamos National Laboratory, Los Alamos, NM, 87545, USA*

[3] *Auburn University, Auburn, AL, U.S.A*

[4] *Laboratorio Nacional de Fusión, CIEMAT, 28040 Madrid, Spain*

[5] *Wigner RCP RMI, Budapest, Hungary*

[6] *Institute for Climate and Energy Research – Plasma Physics, Forschungszentrum Jülich, 52425 Jülich, Germany*

[7] *Princeton Plasma Physics Laboratory, Princeton NJ, 08543, USA*

[8] *Max-Planck-Institute for Plasma Physics, Boltzmannstasse. 2, 85748 Garching bei München, Germany*

Abstract

Wendelstein 7-X (Greifswald, Germany) is an advanced stellarator, which uses the modular coil concept to realize a magnetic configuration optimization for fusion-relevant properties. The magnet system of the machine allows realization of a large diversity of magnetic configurations, having rotational transform at the boundary $\iota/2\pi$ from 5/6 to 5/4. The predecessor experiment, Wendelstein 7-AS, revealed that in low-to-medium density experiments small changes in iota near rational iota values could lead to significant variation of confinement. Configuration scans in the latest W7-X operational campaign aimed to investigate similar effects, varying gradually rotational transform with help of the planar coil currents at the same discharge conditions. This paper presents an overview of experimental results of configuration scans performed between High-iota and Standard reference magnetic configurations. Rotational transform variation revealed an increase of the plasma energy and confinement time in several intermediate limiter configurations. In addition, a change from oscillatory to sawtooth-crashing behavior was observed by several diagnostics, with the mode amplitude correlating with the size of the internal 5/5 islands.

Introduction

Wendelstein 7-X (W7-X) is an advanced stellarator, which uses the modular coil concept to realize a magnetic configuration optimization for fusion-relevant properties like MHD-equilibrium and -stability, neoclassical transport in the low-collisionality range, small bootstrap current and favorable fast particle confinement [1]. The machine went into operation in December 2015 at the Max-Planck-Institut für Plasmaphysik in Greifswald, Germany, and in

October 2018 successfully finished the second experimental phase with an uncooled divertor, the so-called Test-Divertor-Unit (TDU) [2]. This phase was devoted to the exploration of divertor operation, of high-performance H2-discharges and to the verification of those optimization principles which have been accessible within the experimental capabilities of the device at this early state of operation.

The magnet system of the machine consists of 50 non-planar (NPC) and 20 planar (PC) superconducting coils, which are arranged in five identical modules. This allows realization of a large diversity of magnetic configurations [3]. Each machine module consists of two flip-symmetric (stellarator-symmetric) half-modules. The variation of the magnetic configurations is made possible by five independently powered distinct NPC and two PC, which are arranged in one half-module. The majority of magnetic configurations have the rotational transform $\iota/2\pi=5/5$ at the boundary with five islands cut by the divertor, and differ in magnetic shear, mirror ratio and the position of the plasma column [4]. Reference Low-iota and High-iota configurations have, respectively, six and four islands outside the last-closed-magnetic-surface and are characterized by $\iota/2\pi=5/6$ and 5/4 respectively.

The predecessor experiment, Wendelstein 7-AS (W7-AS), revealed, that in low-to-medium density experiments small changes in iota near rational iota values could lead to significant variation of confinement [5] in limiter- (when plasma volume is restricted by the divertor plates) and divertor (when divertor plates cut external plasma islands) experiments. Wendelstein 7-AS and Wendelstein 7-X are both low-shear machines, and configuration scans in the latest W7-X operational campaign aimed to investigate effects observed in W7-AS, varying gradually rotational transform with help of the planar coil currents at the same discharge conditions. For this purpose, the configurational space between W7-X High-iota and Standard magnetic configurations was chosen, since the High-iota magnetic configuration has almost a negligible value of the bootstrap current at low densities [6], and, hence, one can more easily differentiate between various possible impacts on confinement properties excluding the influence of the bootstrap current on the rotational transform.

Technical realization of configuration scans and configuration modifications

High-iota magnetic configuration, further configuration A (Table 1 shows the short abbreviations used for the better readability and internal configuration naming according to W7-X specification), is characterized by negative identical coil currents of approximately -10 kA per winding (in each of 36 windings) in each PC, having identical non-planar coil currents of approximately 14 kA per winding (in each of 108 windings). Nominal Standard magnetic configuration, further configuration M, is characterized by identical currents of approximately 13 kA per winding in all NPCs, having zero currents in PCs. In order to compensate for the change of iota due to the coil deformations under electromagnetic loads [7], the nominal planar coil currents had to be reduced by 250 A in all experimentally run configurations. The configuration-scan between configurations A and M was performed by prescribed, different in each configuration, PC currents. The NPC currents in each intermediate magnetic configuration were slightly adjusted in order to fulfill resonant conditions for the ECRH heating, maintaining

2.52 T magnetic field in the bean-shaped cross-section. To ensure the reliable machine operation in all intermediate magnetic configurations the structural analysis was performed with help of the ANSYS code, verifying whether the values of several crucial mechanical parameters stay within the safety limits [8]. Coil currents, experimental IDs and some characteristic parameters of the scanned magnetic configurations, discussed in this article, are summarized in Table 1. During configuration-scan experiments, trim coils were also in use in order to compensate for field errors and to symmetrize divertor loads [9], but due to their negligible impact on the magnetic field they were not taken into account in the calculations.

Figure 1 shows Poincaré plots characterizing topological changes during configuration scans. The chain of external 5/4 islands, cut by TDU in A configuration, is gradually displaced outwards in subsequent magnetic configurations, turning into limiter configurations starting with the configuration C. At the same time the chain of 5/5 internal islands appears in the center of the plasma, gradually moving to the boundary with the change of PC currents towards the outer 5/5 island chain in the configuration M, where they are cut by the divertor. In addition, intermediate configurations have a chain of 10/11 islands. Figure 2 (upper figure) demonstrates rotational transform profiles in all scanned configurations.

For a comprehensive comparison of different configuration-scan experimental programs, it was intended to achieve identical input conditions in all of them. During the experimental session from 2018.09.27, the input configuration scan discharge parameters – the ECRH power and the electron density were kept at the level P_{ECRH} =2 MW and n_e =3.5 e19 m^{-3} respectively. The typical discharge duration was 4 seconds, which was chosen as a compromise between technical restrictions due to the 8 MJ total energy limit, prescribed for all new (not run in the previous experimental sessions) configurations, and physical needs to provide constant profiles at multiple energy confinement times. Figure 3 shows a typical configuration scan discharge. In addition, two discharges with high density, achieved by the pellet injection, were performed in the I and L configurations.

Confinement evaluation during configuration scans

The main parameter characterizing plasma confinement during configuration scans was the diamagnetic energy. Figure 4 demonstrates the time traces of the measured diamagnetic energy and the plasma volume in all scanned configurations, calculated from the Fourier representation of the cylindrical coordinates describing the last-closed-magnetic-surface, obtained by field-line tracing. The diamagnetic energy was continuously increased starting with the magnetic configuration A up to the intermediate J configuration, and afterwards consistently decreased towards the M configuration.

In order to confirm the tendency in the observed confinement properties, VMEC [10] and V3FIT [11] calculations were performed. VMEC calculations used fitted plasma pressure profiles, based on the measurements of the electron density, electron and ion temperature as well as Zeff values. The discharge time point of 3.5 s was chosen for the comparison between different configurations in order to have already equilibrated plasma profiles. The V3FIT equilibrium reconstruction code utilized only magnetic diagnostics signals, including

compensation loops, segmented Rogowski and saddle coils. Although the main part of intermediate configurations had “limiter plasmas”, one can exclude the dependency on volume completely by normalizing of energy values to the configuration volume. Figure 5 shows the corresponding normalized values of the diamagnetic and kinetic energy as a function of rotational transform in the center: black dots demonstrates the diamagnetic energy, red – kinetic energy obtained from VMEC evaluations, green – V3FIT kinetic energy reconstruction. The shaded area shows the diamagnetic energy error bars, which can be estimated as +-5% from the measured value in all experiments [12]. The vertical blue lines are the combined estimates of the errors, corresponding to the pressure profile fits and diagnostic measurements, used for the reconstruction of the pressure profiles. This error estimates are based on the Gaussian uncertainty propagation. Figure 6 shows the reconstructed pressure profiles as a function of an effective plasma radius, used in VMEC calculations. For a better readability, only five configurations selected in Figure 1 are shown, where A and M are starting and final configurations in the scans, C and K are first and last limiter (with the same volume) configurations and J is the configuration with the maximum value of the normalized plasma energy.

Results presented in Fig. 5 and 2 (lower figure) show that the increase of the diamagnetic energy in the scanned intermediate configurations occurs due to change of the pressure profiles and is not due to the volume effect. The plasma pressure gradually increases up to the configuration J (ca. 20% difference between normalized Wdia values in limiter C and J configurations) and then decreases in the following configurations up to the configuration M. The comparison of two high performance experimental programs shows ca. 17% difference between normalized Wdia values in I and L configurations, although one has to take into account that these two experimental programs had not identical experimental conditions.

Mode observations during configuration scans

Starting from the configuration C, a special behavior of many diagnostic signals (e.g., segmented Rogowski coils, soft X-ray tomography system, correlation reflectometry, video diagnostics) was observed, related to the mode activity developed apparently in limiter configurations during configuration scans [13]. This mode behavior increased up to the intermediate configuration J, having the maximum normalized diamagnetic energy, and monotonically decreased for the subsequent configurations in the scan. Fig. 7 demonstrates the difference in segmented Rogowski coil signals during configuration scans.

The hypothesis whether the observed mode behavior relates to the size of the internal 5/5 islands, appearing in the intermediate scanned configurations within the last closed magnetic surface, and whether the size of these islands would influence the confinement properties, was checked in the experimental session held in the same experimental campaign 2018.10.17. Several discharges with different control coil currents (I_{cc}), and consequently with a different size of internal islands, were conducted at the same discharge conditions (P_{ECRH} and n_e) with NPC and PC coil currents corresponding the original configuration I (Table 1). Figure 8 demonstrates the measured diamagnetic energy and the electron density. The configuration N

(shown in black color) had zero control coil currents and reproduced the conditions of the configuration scan experimental session from 2018.09.27. The configurations O and P (shown in blue and magenta) had respectively negative and positive control coil currents. In the configuration O with I_{cc}= -1000 A the size of 5/5 islands were significantly reduced. The configuration P had positive control coil currents of 1000 A, which aimed to increase the 5/5 island size. The average value of the diamagnetic energy stayed in these three experiments almost at the same level independently of the island size. The small differences in the absolute values were caused by insignificant changes of the electron density (Fig. 8). At the same time the mode activity was completely different in these discharges. It grew with the increase of the island size, and decreased with the island size reduction, which was detected by various diagnostics, for example, by ECE [14] observations shown in Figure 9.

Discussion

To exclude the influence of mapping on evaluation results the sensitivity analysis of plasma pressure profiles was performed. Fig. 2 (lower figure) shows already mapped and fitted pressure profiles, where the outliers of the Thomson scattering data were excluded. Usually pre-calculated vacuum equilibria (with beta=0%) are taken to map raw experimental density and temperature data. Sensitivity studies performed for the mapping of the experimental data with different finite-beta equilibria revealed almost no difference in the mapping results with beta=0% and beta=0.44% as well as in the mapping results with equilibria based on different theoretical pressure shapes (Figure 6). This can be explained by the rather low average beta values in all configurations-scan discharges (around 0.3%).

Conclusions

In the latest W7-X divertor operation experimental campaign, configuration scans were conducted between W7-X High-iota and Standard reference magnetic configurations by means of planar coil current change over iota-range of 0.16 w.r.t. the rotational transform value in the center. The scans consisted of a set of 13 experimental programs with very similar plasma parameters but a varied magnetic configuration (rotational transform). Rotational transform variation revealed an increase of the plasma energy and confinement time in several intermediate limiter configurations, caused by an increase of the plasma pressure (the effect of plasma volume was taken into account).

In addition, the ELM-like mode behavior was observed by several diagnostics in the intermediate limiter configurations. The mode amplitude correlates with the size of the internal 5/5 islands: it becomes larger with the island enlargement and decreases with the reduction of the island size. The change of the island size seems to have no effect on the diamagnetic energy, however, which was experimentally proven in the discharges with the identical density and heating power in one of scanned limiter configurations.

Future studies should include the precise characterization of the observed modes as well as the evaluation of the inversion radius (and, hence, location) of the modes. The experimental exploration of the “improved” intermediate configurations at higher beta values is in planning

for the next W7-X experimental campaigns. In addition, the configuration scans need to be complemented by discharges in other, not yet scanned intermediate magnetic configurations between High-iota and Standard reference configurations and compared with configurations scans between Low-iota and Standard reference configurations. Another interesting task would be to investigate the influence of island topology changes on the confinement properties and the mode behavior. The improvement of basic diagnostic abilities can help to analyze profile effects in more detail in the next experimental campaigns.

References

1. G. Grieger, et al., “Modular stellarator reactors and plans for Wendelstein 7–X”, Fusion Technol. 21 (1992) 1767-1778.
2. T. Klinger, et al., “Overview of first Wendelstein 7-X high-performance operation”, Nuclear Fusion 59 112004 (2019).
3. T. Andreeva, et al., “Characteristics of main configurations of Wendelstein 7-X”, Problems of Atomic Science and Technology, Series: Plasma Physics, Vol. 4 (2002) 45-47.
4. J. Geiger, et al. “Physics in the magnetic configuration space of W7-X”, Plasma Phys. Control. Fusion 57 (2015) 014004 (11pp).
5. M. Hirsch, et al., “Major results from the stellarator Wendelstein 7-AS”, Plasma Phys. Control. Fusion 50 (2008) 053001 (204pp).
6. T. Andreeva, et al., “Equilibrium evaluation for Wendelstein 7-X experiment programs in the first divertor phase”, Proc. 30th Symposium on Fusion Technology, Giardini Naxos, Sicily (2018).
7. T. Andreeva, et al., “Influence of deviations in the coil geometry on Wendelstein 7-X plasma equilibrium properties”, Proc. 29th Symposium on Fusion Technology, Prague, Czech Republic (2016).
8. V. Bykov, et al., “Engineering Challenges of Wendelstein 7-X Mechanical Monitoring during Second Phase of Operation”, Fusion Science and Technology (2019), 730-739, DOI: 10.1080/15361055.2019.1623568.
9. Samuel A. Lazerson, et al., Plasma Phys. Control. Fusion 60 (2018) 124002 https://doi.org/10.1088/1361-6587/aae96b
10. S. Hirshman, W. van Rij, P. Merkel, “Three-dimensional free boundary calculations using a spectral Green's function method”, Comput. Phys. Comm., 43 (1986), 143-155.
11. J.D. Hanson, D.T. Anderson, M. Cianciosa, et al., “Non-axisymmetric equilibrium reconstruction for stellarators, reversed field pinches and tokamaks”, Nuclear Fusion 53 083016 (2013).
12. K. Rahbarnia, et al., “Diamagnetic energy measurement during the first operational phase at the Wendelstein 7-X stellarator”, Nuclear Fusion 58 096010 (2018).
13. G. Wurden, et al., “Structure of island localized modes in Wendelstein 7-X”, Proc. 46th EPS Conference on Plasma Physics, Milan, Italy (2019).
14. M. Hirsch, et al., “ECE Diagnostic for the initial Operation of Wendelstein 7-X”, EPJ Web of Conferences 203, 03007 (2019).

FIGURES AND TABLES

name	experimental ID	W7-X spec.	NPC current [A]	PC current [A]	CC current [A]	ι/2π(0)	volume [m3]	Wdia @3.5 s [kJ]
A	20180927.09	FTM001+252	14219	-10040	0	1.012	25.64	288
B	20180927.15	FQM001+252	13883	-7290	0	0.965	31.22	309
C	20180927.16	FOM003+252	13608	-5040	0	0.928	31.45	334
D	20180927.17	FNM+252	13577	-4790	0	0.924	31.66	343
E	20180927.18	FNM001+252	13546	-4540	0	0.920	32.06	354
F	20180927.19	FNM002+252	13515	-4290	0	0.916	32.24	361
G	20180927.20	FMM+252	13485	-4040	0	0.912	32.41	367
H	20180927.21	FMM001+252	13454	-3790	0	0.908	31.92	397
I	20180927.22	FMM002+252	13423	-3540	0	0.904	32.61	399
J	20180927.28	FMM003+252	13392	-3290	0	0.900	32.61	445
K	20180927.29	FLM+252	13361	-3040	0	0.897	32.67	419
L	20180927.30	EJM+252	13114	-1040	0	0.862	27.76	293
M	20180927.33	EJM004+252	13016	-250	0	0.854	30.46	321
N	20181017.21	FMM002+252	13423	-3540	0	0.904	32.61	495
O	20181017.23	FMM002+252	13423	-3540	-1000	0.904	32.61	459
P	20181017.24	FMM002+252	13423	-3540	1000	0.904	32.61	463

Table 1: Configuration naming in the article, their experimental IDs, configuration names according W7-X internal specification, non-planar-, planar- and control coil currents in scanned configurations in two experimental sessions discussed, rotational transform value in the center volume of scanned configurations and diamagnetic energy measured at 3.5 s.

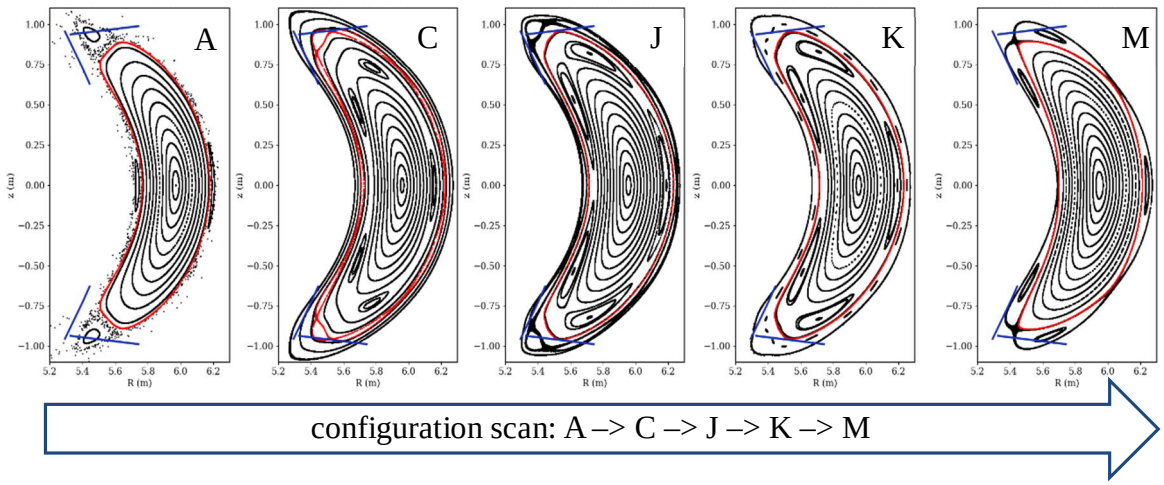

Fig.1. Poincaré plots reflecting the modification of magnetic configurations during the configuration scan, red color indicates the last-closed-magnetic-surface.

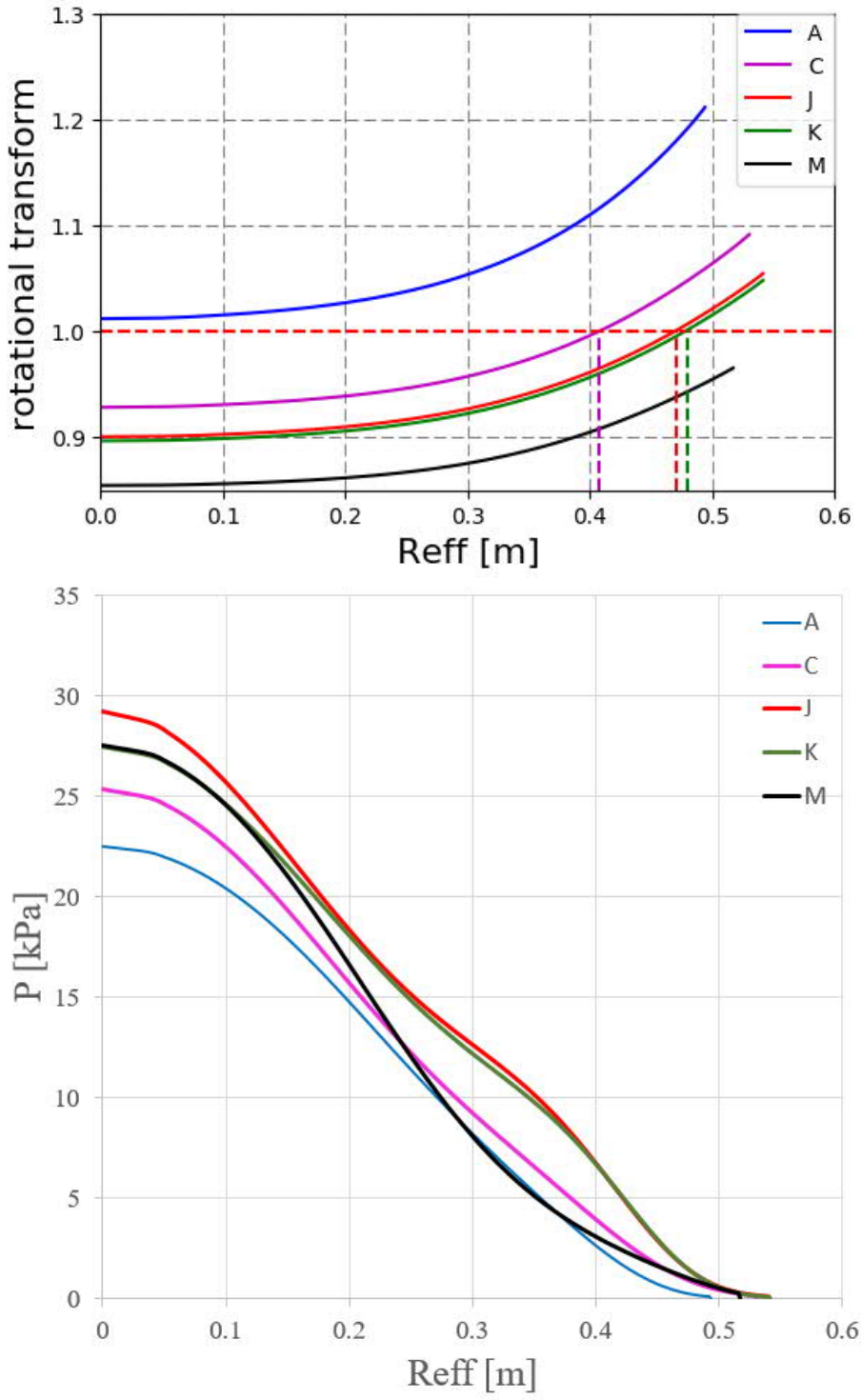

Fig. 2. Upper figure: Rotational transform in configurations shown in Fig.1. The red horizontal dashed line shows ι/2π=5/5. Vertical dashed lines show Reff of the internal 5/5 islands in scanned configurations selected in Fig.1. Lower figure: pressure profile fits used in VMEC calculations for configurations presented in Fig.1. The last point of each curve indicates the position of the LCMS.

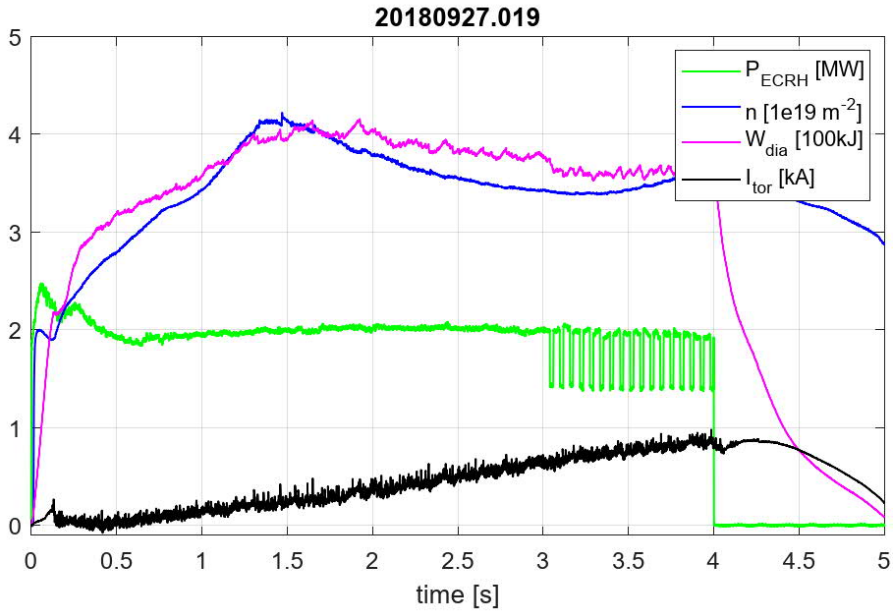

Fig. 3. Typical time traces of plasma parameters during configuration scans.

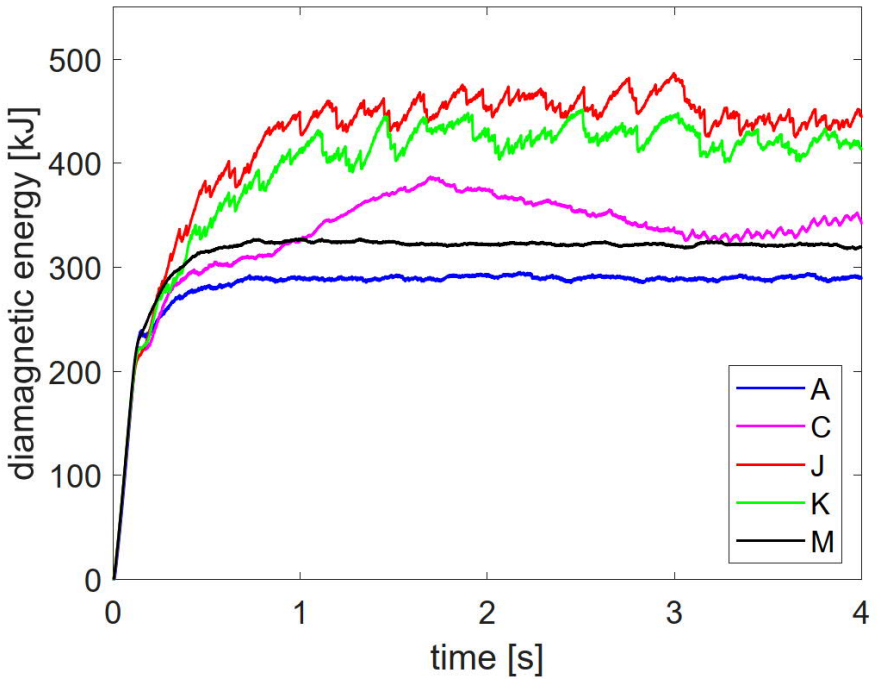

Fig. 4. Diamagnetic energy measured in configuration scans as well as the corresponding plasma volumes and internal names of scanned configurations.

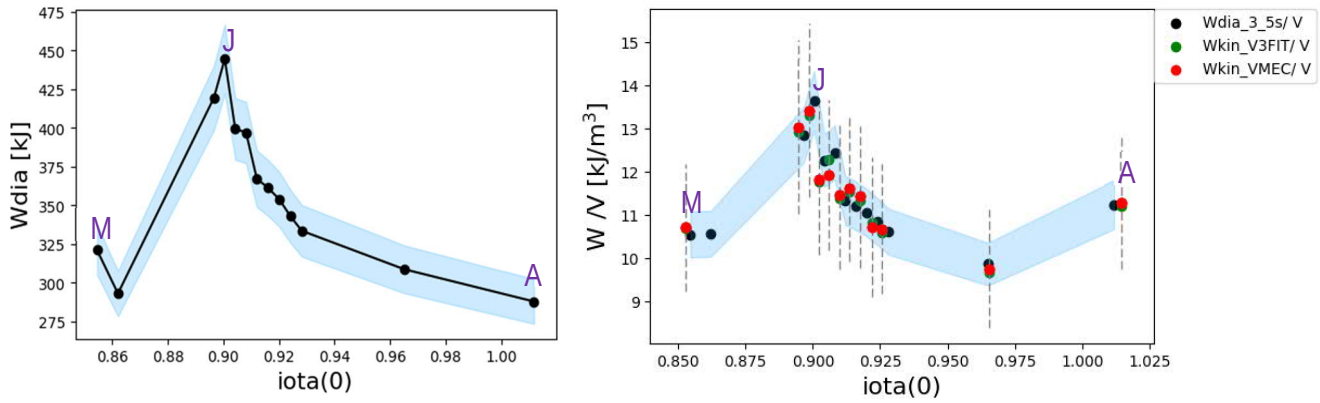

Fig. 5. Left figure: normalized measured diamagnetic (black) and evaluated kinetic energy (red, green), including error bars. Blue shaded area indicates the measurement errors in the diamagnetic energy. Right figure: measured diamagnetic energy (black) without normalization and corresponding measurement errors (blue shaded area).

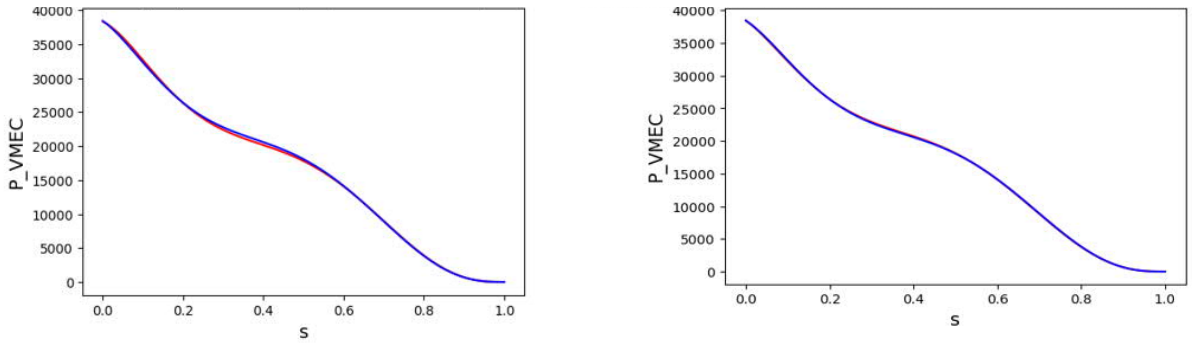

Fig. 6. Left figure: difference in the pressure profile, mapped with pre-calculated equilibria with β=0% (red line) and β=0.44% (blue line) for FMM002+252 configuration. Right figure: difference in the reconstructed pressure profile, mapped with pre-calculated equilibria with the parabolic pressure profile (red line) and the pressure profile with the peaking factor 3 (blue line) for FMM002+252 configuration.

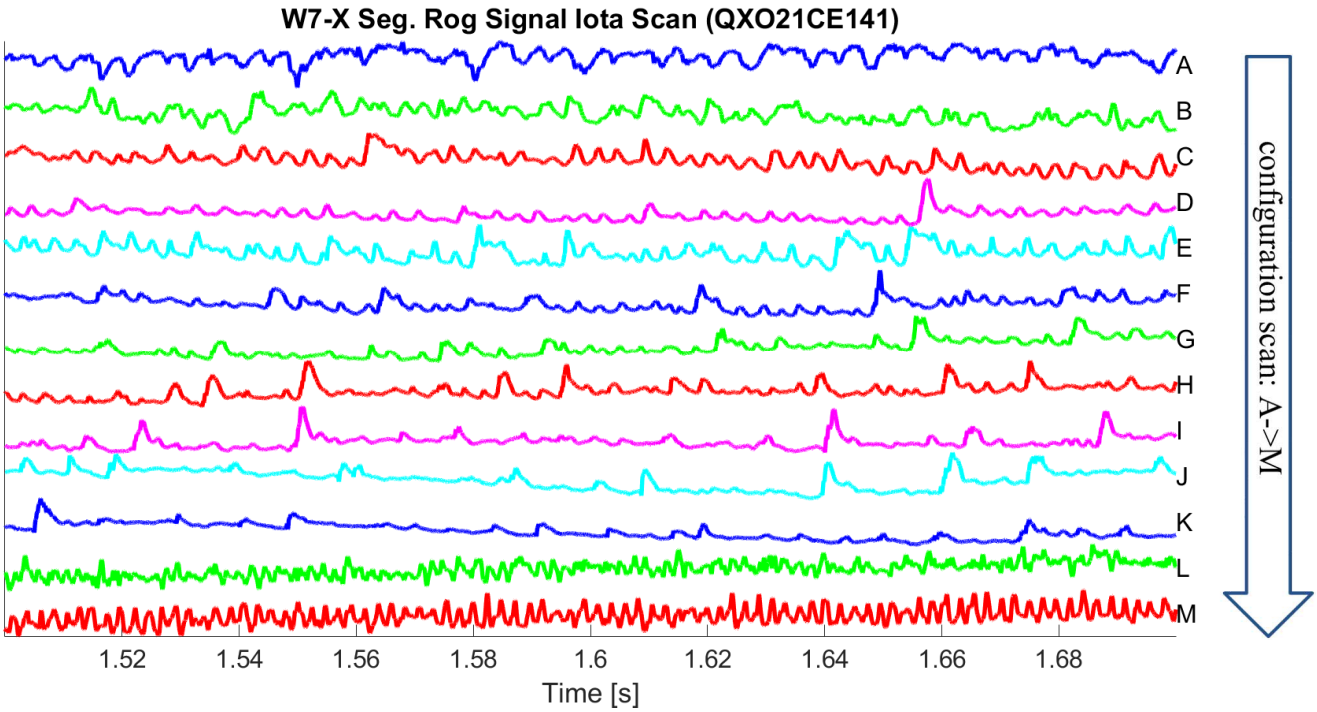

Fig. 7. Segmented Rogowski coil signals during configuration scans.

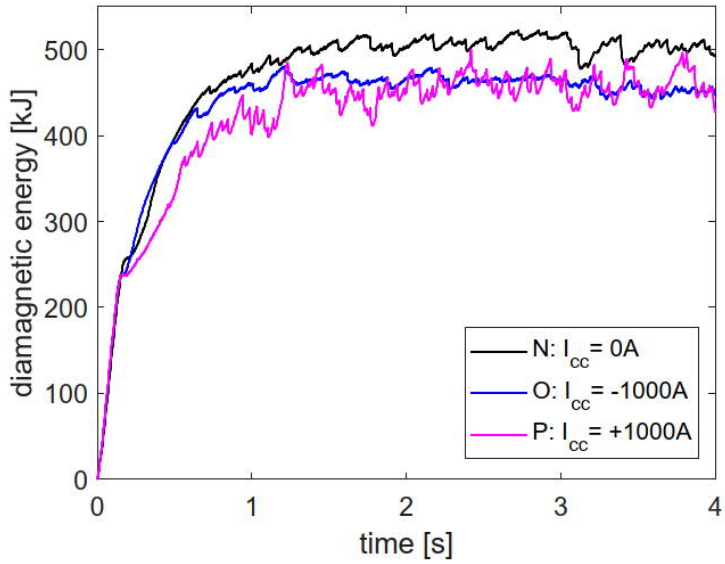

conf.	W_{dia} [kJ]	$n_e \cdot [10^{19}/m^3]$	W_{dia}/n_e [kJ/$10^{19}/m^3$]
N	503	6.7	75.1
O	462	6.1	75.7
P	454	6.0	75.7

Fig. 8. Influence of the m/n=5/5 island chain size in one the intermediate limiter configurations. Similar discharges on separate days indicate high level of reproducibility of the discharge conditions. Mode activity decreases when the island size is reduced (I_{CC}=-1000 A) and changes character when the island size is increase (I_{CC}=+1000 A).

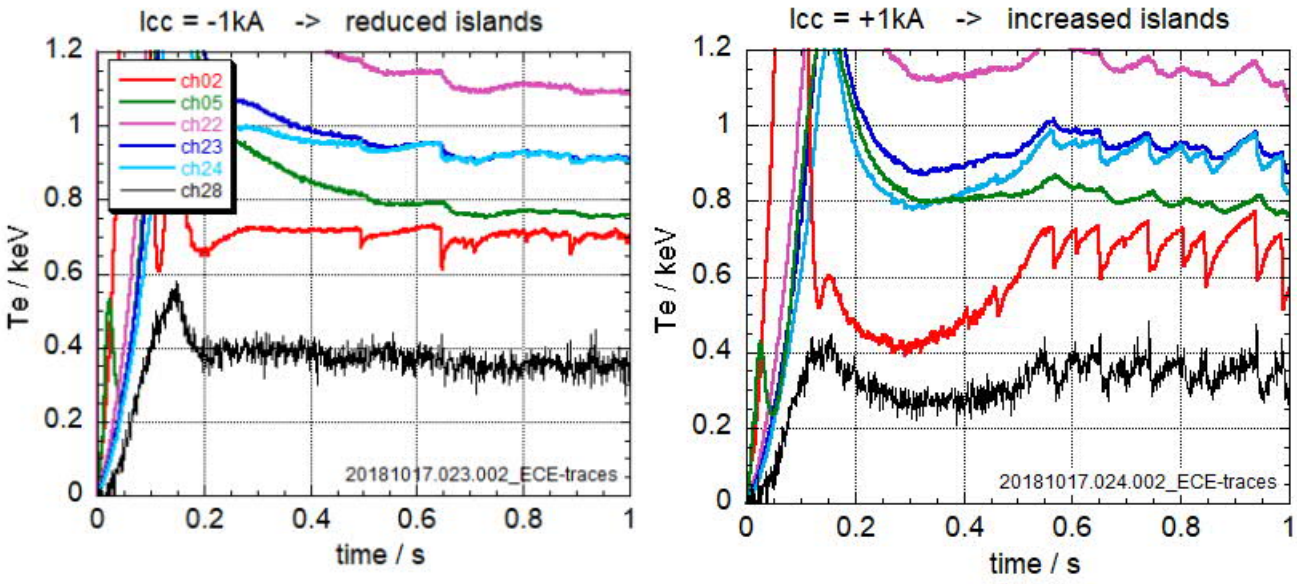

Fig. 9. ECE observations in discharges with the decreased (left) and increased (right) island size (FMM002+252 configuration).